# Serial activation of distinct cytoarchitectonic areas of the human S1 cortex after posterior tibial nerve stimulation

Isao Hashimoto,[1,2,CA] Kenji Sakuma,[2] Tomoaki Kimura,[3] Yoshinobu Iguchi[4] and Kensuke Sekihara[5]

[1]Human Information Systems Laboratory (Tokyo Office), Kanazawa Institute of Technology, 6-7-8 Akasaka, Minato-ku, Tokyo 107-0052; [2]Department of Integrative Physiology, National Institute for Physiological Sciences, Okazaki; [3]Department of Acupuncture, Tsukuba College of Technology, Tsukuba; [4]Department of Psychophysiology, Tokyo Institute of Psychiatry, Tokyo Metropolitan Organization for Medical Research, Tokyo; [5]Department of Electronic Systems & Engineering, Tokyo Metropolitan Institute of Technology, Tokyo, Japan

[CA,1]Corresponding Author and Address

Received 6 April 2001; accepted 11 April 2001

MEG recordings visualized non-invasively a dynamic anterior–posterior activation in the pyramidal cell population of the human primary somatosensory cortex (S1) after posterior tibial nerve stimulation. Somatosensory evoked fields (SEFs) were recorded over the foot area in response to right posterior tibial nerve stimulation at the ankle in six normal subjects. A newly developed MEG vector beamformer technique applied to the SEFs revealed two distinct sources in the mesial wall of the left hemisphere around the primary P37m response typically separated by 1.3 cm. The first source was located in area 3b and oriented toward the contralateral hemisphere. The second source was assumed to be in an area near the marginal sulcus and the source orientation was directed posteriorly. The first source began to be active during the initial slope of the P37m. The second source was active after the P37m peak and the signal intensities of the first and second sources were equal at a mean latency of 2.6 ms after the peak of P37m. Then the first source became inactive and the second source was dominant after about 5 ms post-P37m peak. These findings suggest that a single peaked posterior tibial nerve P37m consists of partially overlapping two subcomponents generated in area 3b and an area near the marginal sulcus. *NeuroReport* 12:1857–1862 © 2001 Lippincott Williams & Wilkins.

**Key words**: Area 3b; Marginal ramus of cingulate sulcus; MEG vector beamformer technique; P37m; Posterior tibial nerve; Somatosensory evoked fields; Two distinct sources

## INTRODUCTION

MEG signals measured outside the head are generated primarily from cortical currents tangential to the scalp. Since MEG signals mainly reflect intracellular current flow within the apical dendrites of the cortical pyramidal cells, only activity of pyramidal neurons in the cortical fissures can be detected. In other words, activity of a large area of the cortical gyri remains undetected due to its radial current flow. However, there is one exception to this general rule; in the mesial surface of the brain, intracellular currents in cortical fissures and gyri are both tangential to the scalp and can be recorded. Thus, this cortical area of paracentral lobule receiving projections mainly from the foot is uniquely situated for the MEG study of early somatosensory information processing.

However, considerable interindividual anatomical variations have been documented for the superior end of the central sulcus; the central sulcus extends to the medial surface in 64% of cases, just reaches the superior margin of the hemisphere in 16%, and in 20 % it does not even reach the superior margin [1]. These morphological variations of the foot area of somatosensory cortex have been further substantiated by recordings of cortical somatosensory evoked potentials (SEPs) after stimulation of the posterior tibial nerve in which locations exhibiting maximum P37 amplitude distributed widely within the paracentral lobule [2]. By recording somatosensory evoked fields (SEFs) to posterior tibial and sural nerves, Huttunen *et al.* [3] observed the changing field patterns with temporally shifting orientations of the source currents during various components within 200 ms. Similar orientation changes were reported during P37m in which the field patterns to the posterior tibial nerve stimulation appeared to rotate very quickly (15°/ms) as a function of time [4]. These orientation changes were interpreted as successive activation of different cytoarchitectonic areas in the foot primary somatosensory cortex (S1) [4,5]. In the studies above, source currents were modeled with a single moving dipole.

Hari *et al.* [6] examined in more detail activation patterns of the human foot S1 cortex by application of a two-dipole time-varying source model. The findings suggested that areas 3b and 5 were sequentially activated.

However, there has been no report in support of or against the observed sequential activation for posterior tibial nerve stimulation. The MEG vector beamformer technique recently developed by Sekihara *et al*. [7,8] provides us with a unique tool for the analysis of multiple sources located nearby, which are activated simultaneously and/or successively. In the present study, the P37m component for stimulation of posterior tibial nerve was characterized by applying the beamformer technique. We found that two distinct sources separated by about 1.3 cm were sequentially and simultaneously active during the P37m primary response. The results using a single moving dipole model were reported previously [9].

## MATERIALS AND METHODS

Six healthy adults (three females, three males; age 25–30 years, mean 28) were studied. Informed consent was obtained prior to the study. Brief electrical stimuli with 0.2 ms duration were delivered to the right posterior tibial nerve at the ankle (cathode proximal) with a repetition rate of 4 Hz. The stimulus intensity was three times sensory threshold and elicited a mild twitch of toe. Magnetic recordings (bandpass 0.1–1200 Hz) were taken from the vertex centering at Cz of the international 10-20 system with a 37-channel SQUID gradiometer (BTi Magnes, San Diego, CA) in a magnetically shielded room. The detection coils of the gradiometer are arranged in a uniform, concentric array on a spherical surface with a radius of 122 mm; each coil measures 20 mm in diameter. The sensors are configured as first-order axial gradiometers with a baseline of 50 mm. The field sensitivities of the sensors were 10 fT/$\sqrt{}$Hz or better.

An epoch of 60 ms duration (10 ms pre- and 50 ms post-stimulus) was digitized at a 4000 Hz/channel sampling rate and 10 000 responses were averaged off-line. DC offset was based on the pre-stimulus period.

The origin of the head-based co-ordinate system was defined as the midpoint between the pre-auricular points. The x-axis pointed from the origin to the nasion, the y-axis to the left pre-auricular point, and the z-axis to the vertex in a direction perpendicular to the x-y plane. Magnetic resonance imaging (MRI) was acquired with spherical lipid markers (5 mm diameter) placed on the MEG fiduciary points to allow for superposition of source locations onto the MRI slices. A local spherical model was fitted to the digitized head shape over the recording area for each subject.

***Data analysis:*** The MEG vector beamformer technique was applied to localize sources from the P37m component. The results of the analysis were shown as current-density maps for transverse, coronal and sagittal sections of the generic head. Furthermore, the highest current sources for the two activation areas were overlaid on the MRI slices.

The details of this vector beamformer technique have been reported elsewhere [7,8], so it is only briefly described here. Let us define the magnetic field measured by the mth sensor at time t as $b_m(t)$, and a column vector $\mathbf{b}(t) = [b_1(t),...,b_m(t)^T$ as a set of measured data. Here M is the total number of sensors and the superscript T indicates the matrix transpose. A spatial location (x,y,z) is represented by a three-dimensional vector $\mathbf{r}$: $\mathbf{r} = (x,y,z)$. The source moment magnitude at $\mathbf{r}$ and time t is defined as a three-dimensional vector $\mathbf{s}(r,t) = [s_x(\mathbf{r},t),s_y(\mathbf{r},t),s_z(\mathbf{r},t)]$. The estimate of the source moment is denoted as $\hat{\mathbf{s}}(\mathbf{r},t)$. We define $l^x_j(\mathbf{r})$, $l^y_j(\mathbf{r})$ and $1^z_j(\mathbf{r})$ as the jth sensor output when a single source exists at $\mathbf{r}$ with the unit moment directed in the x, y, and z directions, respectively. We then define the lead field matrix $\mathbf{L}(\mathbf{r})$ as a matrix whose jth row is equal to $[l^x_j(\mathbf{r}),l^y_j(\mathbf{r}),^z_j(\mathbf{r})]$; this lead field matrix represents the sensitivity of the whole sensor array at $\mathbf{r}$.

The vector beamformer technique reconstructs the source moment by applying the following linear operation:

$$\hat{\mathbf{s}}(\mathbf{r}, t) = \mathbf{W}^T(\mathbf{r})\mathbf{b}(t) \quad (1)$$

where the matrix $\mathbf{W}(\mathbf{r})$ is a weight matrix defined as $\mathbf{W}(\mathbf{r}) = [\mathbf{w}_x(\mathbf{r}),\mathbf{w}_y(\mathbf{r}),\mathbf{w}_z(\mathbf{r})]$, and the weight vectors $\mathbf{w}_x(\mathbf{r})$, $\mathbf{w}_y(r)$ and $\mathbf{w}_z(\mathbf{r})$ detect the x, y, and z components of the source moment, respectively. Let us define the measurement covariance matrix as $\mathbf{D}$, and define the three-dimensional unit column vector as $\mathbf{f}_x$, $\mathbf{f}_y$, and $\mathbf{f}_z$. The weight vectors in an intermediate stage are first obtained using

$$\overline{\mathbf{w}}_\mu(\mathbf{r}) = \frac{\mathbf{D}^{-1}\mathbf{L}(\mathbf{r})[\mathbf{L}^T(\mathbf{r})\mathbf{D}^{-1}\mathbf{l}(\mathbf{r})]\mathbf{f}_\mu}{\sqrt{\mathbf{f}^T{}_\mu\Omega\mathbf{f}_\mu}} \quad (2)$$

where $\boldsymbol{\mu} = x$, y, or z, and

$$\Omega = [\mathbf{L}^T(\mathbf{r})\mathbf{D}^{-1}\mathbf{L}(\mathbf{r})]^{-1}\mathbf{L}^T(\mathbf{r})\mathbf{D}^{-2}\mathbf{L}(\mathbf{r})[\mathbf{L}^T(\mathbf{r})\mathbf{D}^{-1}\mathbf{L}(\mathbf{r})]^{-1}$$

Let us define $\mathbf{E}_s$ as a matrix whose columns consist of the signal-level eigenvectors of $\mathbf{D}$. Then, the final form of the weight vectors are obtained by projecting the weight vector $e_\mu$ onto the signal subspace of the measurement covariance matrix, i.e.

$$\mathbf{w}_\mu(\mathbf{r}) = \mathbf{E}_s\mathbf{E}^T{}_s\overline{\mathbf{w}}_\mu(\mathbf{r}). \quad (3)$$

Then the source moment at $\mathbf{r}$ is estimated using eqn (1) with the weight vectors obtained using eqns (2) and (3). Note that when calculating the above weight vectors, the location $\mathbf{r}$ is a controllable parameter. Therefore, the source-moment distribution can be reconstructed by scanning the beamformer output over the region of interest in a completely post-processing manner. Because this reconstruction is performed at each instant in time, the spatio-temporal reconstruction of the source activities can be obtained.

## RESULTS

Figure 1 illustrates P37m in an extended time scale (upper traces) recorded over foot somatosensory region in the left hemisphere. The magnetic signals start 30 ms after the right posterior tibial nerve stimulation. The P37m peak occurs at 34 ms. The current–density maps produced by application of the beamformer technique to the MEG data revealed initial activation in the anterior part of S1 foot area at 33.1 ms (a sampled point shown by a red dotted line on the superimposed SEF traces at the top), followed by co-activation of the posterior part of S1 cortex at 36.2 ms (indicated by a green line; Fig. 1). At 1 ms later (37.2 ms), the posterior activation became dominant (indicated by a blue line) and at about 2 ms thereafter (39.1 ms, black line),

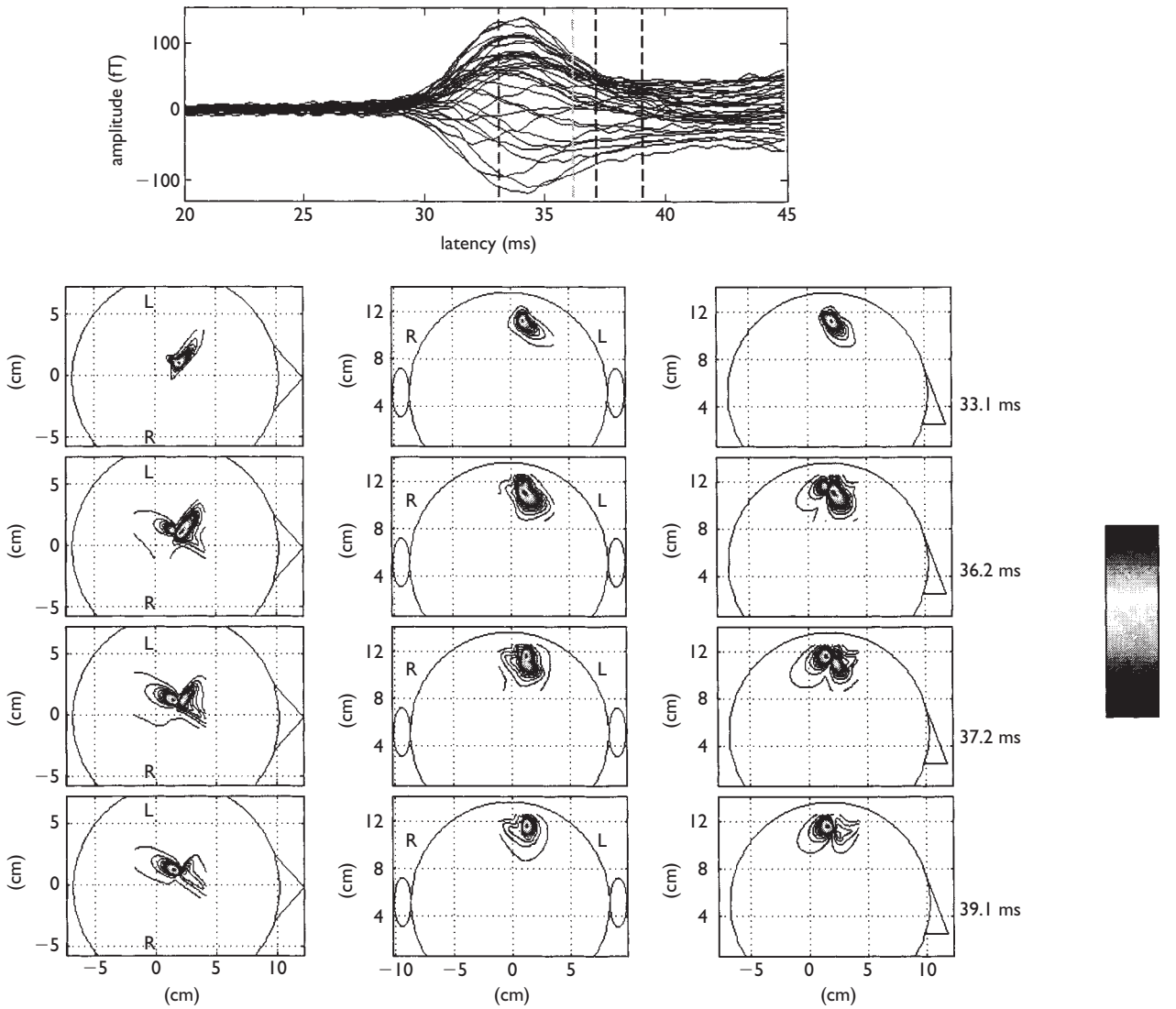


**Fig. 1.** Current–density maps during P37m for right posterior tibial nerve stimulation in one subject. Superimposed traces at the top of the figure illustrate P37m in an extended time. The contour maps show reconstructed source magnitude distributions at four different latencies. The reconstruction grid spacing was set at 1 mm. The maximum intensity projections onto the axial (left column), coronal (middle column), and sagittal (right column) directions are shown. The letters L and R in the coronal views indicate the left and right hemispheres, respectively. The circles depicting a human head show the projections of the sphere used for the forward modeling. The colors of contours represent the relative intensity of the source magnitude; the relationship between the colors and relative intensities is indicated by the color bar. The current-density maps revealed initial activation in the anterior part of SI foot area at 33.1 ms (a sample point shown by a red dotted line on the SEF traces at the top), followed by co-activation of the posterior part of S1 cortex at 36.2 ms (indicated by a green line). At 1 ms later (37.2 ms), the posterior activation became dominant (indicated by a blue line) and at about 2 ms thereafter (39.1 ms, black line), the initial anterior activation completely disappeared.

the initial anterior activation completely disappeared (Fig. 1). In all subjects, anterior activation was followed by posterior activation. Thus, the intensities of the two sources varied as a function of time. Figure 2 shows co-registration of MEG sources and MRI in which the anterior source was in area 3b and the posterior source was in an area near the marginal sulcus (marginal ramus of the cingulate sulcus).

The spatial and temporal relations between the two sources are summarized in Table 1. In order to facilitate comparison between individual subjects with different lengths of conduction pathways, the time origin was set at the peak of P37m. Similarly, the spatial origin was set at the location of the anterior source with the highest current source density. With these normalization processes, large interindividual anatomical variations documented for the central sulcus and the marginal sulcus with respect to the head co-ordinate system can be minimized. The average latency ($\pm$ s.d.) when the intensities of the two sources were equal was $2.6 \pm 2.4$ ms after the peak of P37m. The latency when the anterior source disappeared and only the posterior source was present was $5.0 \pm 3.1$ ms following the P37m peak. Compared with the early anterior source, the

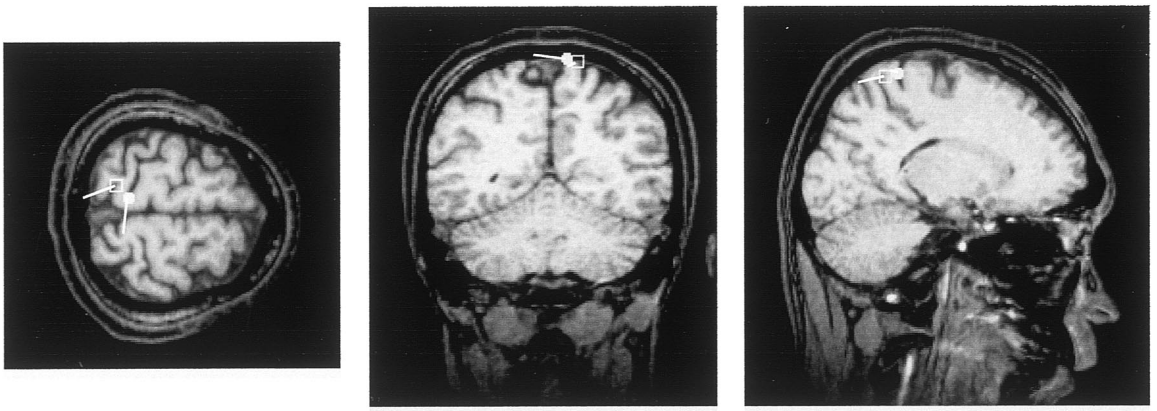

**Fig. 2.** Superimposition of P37m sources on MRI for the data presented in Fig. 1. The anterior source indicated by a solid circle was in area 3b, and the posterior source indicated by a square was in an area near the marginal sulcus (marginal ramus of the cingulate sulcus). The bars originating from the source locations indicate the moment directions of these sources. From the left to right are axial, coronal and sagittal slices of the MRI. On the coronal slice, left hemisphere is shown on the right as in Fig. 1.

**Table 1.** Spatial and temporal relationships between the anterior and posterior sources during P37m for posterior tibial nerve stimulation.

| Subject | Latency[a] when the two sources are equal in intensity (ms) | Latency[a] when only the posterior source is present (ms) | $\Delta x^b$ (mm) | $\Delta y^b$ (mm) | $\Delta z^b$ (mm) | Total[b] distance between the two sources (mm) |
|---|---|---|---|---|---|---|
| 1 | 2.90 | 5.10 | −6.3 | −1.7 | 2.0 | 6.9 |
| 2 | 2.40 | 4.00 | −7.6 | 6.7 | −1.5 | 10.1 |
| 3 | −0.30 | 3.30 | −10.7 | −0.8 | 2.3 | 12.1 |
| 4 | 2.50 | 4.90 | −8.0 | 1.7 | 6.7 | 10.5 |
| 5 | 0.94 | 1.94 | −15.3 | 3.6 | 2.1 | 15.8 |
| 6 | 6.70 | 11.0 | −19.0 | 3.8 | 1.0 | 19.4 |
| Mean | 2.57 | 5.04 | −11.2 | 2.2 | 2.1 | 12.5 |
| s.d. | 2.37 | 3.14 | 5.0 | 3.1 | 2.7 | 4.5 |

[a]The time origin was set at the peak of P37m.
[b]The spatial origin was set at the location of the anterior source.

later posterior source was located $11.2 \pm 5.0$ mm posterior, $2.2 \pm 3.1$ mm lateral, and $2.1 \pm 2.7$ mm higher. The mean total distance between the two sources was $12.5 \pm 4.5$ mm. Table 2 shows orientations of the anterior and posterior sources for all subjects. The mean orientation of the anterior source was directed toward the right hemisphere and that of the posterior source was toward contralateral posterior direction.

## DISCUSSION

Previous MEG studies have shown a systematic rotation of source currents in the foot somatosensory cortex after

**Table 2.** The orientation of the anterior and posterior sources. The x, y, and z components of the normal vectors representing these orientations are shown.

| Subject | Anterior source orientation | | | Posterior source orientation | | | Angle[a] ° |
|---|---|---|---|---|---|---|---|
| | x | y | z | x | y | z | |
| 1 | −0.47 | −0.86 | 0.20 | −0.92 | −0.37 | 0.05 | 41 |
| 2 | −0.17 | −0.97 | 0.15 | −0.95 | −0.26 | −0.16 | 67 |
| 3 | 0.91 | −0.41 | 0.10 | 0.66 | −0.71 | 0.22 | 23 |
| 4 | −0.53 | −0.83 | 0.15 | −0.81 | 0.52 | −0.26 | 92 |
| 5 | −0.66 | −0.75 | 0.05 | −0.88 | −0.22 | −0.43 | 44 |
| 6 | −0.67 | −0.72 | 0.16 | −0.82 | 0.31 | −0.48 | 75 |
| Mean | −0.26 | −0.76 | 0.14 | −0.62 | −0.12 | −0.18 | 57 |
| s.d. | 0.60 | 0.19 | 0.05 | 0.63 | 0.45 | 0.27 | 25 |

[a]The angle between the two orientations.

posterior tibial nerve stimulation [4–6]. For the left posterior tibial nerve stimulation, the rotation was counter-clockwise starting approximately from 9 o'clock, and for the right stimulation it was clockwise beginning at 15 o'clock, suggesting initial activation at the mesial surface of the cortex. The present study supports the above findings. Such observations imply time-varying shifts in the center of gravity of cortical activation in an enfolded cortical surface.

Hari *et al*. [6] studied, posterior tibial nerve SEFs with application of the two-dipole time-varying source model in which the two dipoles with fixed locations and orientations were allowed to change their signal strengths as a function of time. Our data seem to support the above two-dipole assumption for SEFs for the posterior tibial nerve stimulation. However, it is also possible that the assumption of the two dipoles being fixed in locations and orientations may not always be physiologically valid. For example, it has been shown recently that an equivalent current dipole (ECD) for N20m primary response to median nerve [10] or index finger [11] stimulation moves serially from medial to lateral direction in area 3b.

Moreover, in general, it is not possible to detect these two sources by using the two-dipole search method. The prerequisite for the two-dipole method is that two sources must exist at each time point, and this prerequisite was not always met in the posterior-tibial SEFs as we have shown in the present study. For example, in Fig. 1, a single source is present at the latency of 33.1 ms. When we applied the two-dipole search method for the field data at this latency, we obtained one dipole precisely at the location of the peak in the contour map and the other near the center of the sphere with the goodness of fit greater than 0.99. When we applied the two-dipole search method for the data at 36.2 ms, we could successfully obtain two dipoles exactly at the two peak locations in the contour map with the goodness of fit greater than 0.99. However, this success is due to the fact that we know a priori from the beamformer analysis that the two sources exist at this time slice. Without this knowledge, we might set the number of dipoles more than two and such a multi-dipole search would surely give a false source configuration with a high value of goodness of fit. We believe that the multi-dipole search method is hardly an effective method because we must know exactly the value of the model parameter (the number of dipoles), which is generally unknown. On the other hand, the beamformer method can reconstruct the multiple source activities without requiring such information and can be effective in the situations where the multi-dipole method fails.

The MEG vector beamformer technique can provide information on temporal and spatial behavior of multiple nearby sources simultaneously and sequentially active, since this technique is basically free from the constraints of the dipole modeling. The present results are generally in line with the temporal activation patterns of the two sources described by Hari *et al*. [6]; anterior activation precedes posterior activation. However, because of the assumption of fixed dipoles, the relative distance of the two sources was left unknown.

The anatomical distance between the central sulcus and the marginal sulcus is presumably about 1.5 cm [1]. Given that the anterior source is in area 3b, the mean distance of 1.3 cm between the anterior and posterior sources will place the posterior source at or near the marginal sulcus in the area of paracentral lobule. Since the field patterns rotated systematically in previous studies [4–6], it is reasonable to assume activation in a fissure located posterior to the central sulcus. Hari *et al.* [6] speculated that the activation took place in area 5 in the anterior wall of the marginal sulcus. They also argue that area 3b in the mesial wall extends very closely to the marginal sulcus, directly abutting on area 5.

With similar types and density of mechanoreceptors responding to tactile air-puff stimulation of foot [12], as compared with those of the hand [13] and face [14], it is more likely that the S1 area receiving projection from the foot is organized in a similar manner as the hand and face S1 cortex (see Brodmann's map [15] of the mesial wall of the hemisphere). Thus, we suggest that foot S1 area consists of 3a, 3b, 1, and 2, not unlike the hand and face S1. Because the timing of activation of the two sources was only a few ms apart, it is unlikely that somatosensory association area 5 is the generator of the posterior source [16,17]. It is plausible that areas 1 and 2 may be located anterior to or at the marginal sulcus. Furthermore, the rotation phenomenon of the field patterns after posterior tibial nerve stimulation can also be explained by the activity in this sulcus. However, the cytoarchitectonic areas of the human foot S1 have been poorly delineated histologically, and thus the precise cytoarchitectonic area generating the posterior source is still an open question and needs more detailed studies integrating anatomical and neurophysiological data.

## CONCLUSION

The MEG vector beamformer technique applied to SEFs after the posterior tibial nerve stimulation revealed two distinct sources, one in area 3b and another near the marginal sulcus, which are sequentially and simultaneously active during P37m primary response. Because cortical fissures and gyri in the mesial surface of the brain are both tangential to the scalp, this cortical area of paracentral lobule receiving projections mainly from the foot is uniquely situated for the MEG study of early somatosensory processing.

## REFERENCES

1. Ono M, Kubic S and Abernathey CD. *Atlas of the Cerebral Sulci*. Stuttgart: George Thieme Verlag; 1990.
2. Allison T, McCarthy Q, Luby M *et al*. *Electroencephalogr Clin Neurophysiol* **100**, 126–140 (1996).
3. Huttunen J, Kaukoranta E and Hari R. *J Neurol Sci* **79**, 43–54 (1987).
4. Fujita S, Nakasato N, Matani A *et al*. Short latency somatosensory evoked field for tibial nerve stimulation: Rotation of dipole pattern over the whole head. In: Baumgartner C, Deecke L, Stroink G and Williamson SJ, eds. *Biomagnetism: Fundamental Research and Clinical Applications.* Amsterdam: Elsevier, 1995: 95–98.
5. Kakigi R, Koyama S, Hoshiyama M *et al*. *Electroencephalogr Clin Neurophysiol* **953**, 127–134 (1995).
6. Hari R, Nagamine T, Nishitani N *et al*. *NeuroImage* **4**, 111–118 (1996).
7. Sekihara K, Nagarajan SS, Poeppel D *et al*. *NeuroImage* **11**, 485 (2000).
8. Sekihara K, Nagarajan SS, Poeppel D *et al*. *IEEE Trans Biomed Eng* in press.
9. Sakuma K and Hashimoto I. *Neuroreport* **10**, 227–230 (1999).
10. Hashimoto I, Kimura T, Sakuma K *et al*. *Neurosci Lett* **280**, 25–28 (2000).

11. Kimura T and Hashimoto I. *Neurosci Lett* **299**, 61–64 (2001).
12. Hashimoto I, Gatayami T, Yoshikawa K et al. *Exp Brain Res* **88**, 318–325 (1992a).
13. Hashimoto I, Yoshikawa K and Sasaki M. *Exp Brain Res* **73**, 459–469 (1988).
14. Hashimoto I, Gatayami T, Yoshikawa K *et al*. *Exp Brain Res* **88**, 639–644 (1992b).
15. Brodmann K. *Vergleichende Lokalisationslehre der Grosshirnrinde in ihren Prinzipien dargestellt auf Grund des Zellenbaues.* Leipzig: Barth; 1909.
16. Allison T, McCarthy G, Wood C *et al*. *J Neurophysiol* **62**, 711–722 (1989).
17. Forss N, Hari R, Salmelin R *et al*. *Exp Brain Res* **99**, 309–315 (1994).

Acknowledgements: This research was supported by a Grant-in-Aid for Scientific Research from the Ministry of Education, Science and Culture of Japan (09877185) and a Grant-in-Aid of the Japan Medical Association (1998). One of the authors (K.S.) was supported by a research project 'Mind Articulation' sponsored by Japan Science and Technology Corporation.